

Article

Layered Double Hydroxides for Remediation of Industrial Wastewater from a Galvanic Plant

Anna Maria Cardinale ^{1,*}, Cristina Carbone ², Sirio Consani ², Marco Fortunato ¹ and Nadia Parodi ¹

¹ Dipartimento di Chimica e Chimica Industriale, Università di Genova, Via Dodecaneso 31, 16146 Genova, Italy; fortunato.marco@hotmail.it (M.F.); nadia@chimica.unige.it (N.P.)

² Dipartimento di Scienze della Terra, dell'Ambiente e della Vita, Università di Genova, Corso Europa 26, 16132 Genova, Italy; cristina.carbone@unige.it (C.C.); sirio.consani@edu.unige.it (S.C.)

* Correspondence: cardinal@chimica.unige.it; Tel.: +39-10-3536156; Fax: +39-10-3536163

Received: 3 May 2020; Accepted: 28 May 2020; Published: 30 May 2020



Abstract: Owing to their structure, layered double hydroxides (LDHs) are nowadays considered as rising materials in different fields of application. In this work, the results obtained in the usage of two different LDHs to remove, by adsorption, some cationic and anionic pollutants from industrial wastewater are reported. The two compounds MgAl-CO₃ and NiAl-NO₃ have been prepared through a hydrothermal synthesis process and then characterized by means of PXRD, TGA, FESEM, and FTIR spectroscopy. The available wastewater, supplied by a galvanic treatment company, has been analyzed by inductively coupled plasma-optical emission spectrometry (ICP-OES), resulting as being polluted by Fe(III), Cu(II), and Cr(VI). The water treatment with the two LDHs showed that chromate is more efficiently removed by the NiAl LDH through an exchange with the interlayer nitrate. On the contrary, copper and iron cations are removed in higher amounts by the MgAl LDH, probably through a substitution with Mg, even if sorption on the OH⁻ functional groups, surface complexation, and/or precipitation of small amounts of metal hydroxides on the surface of the MgAl LDH could not be completely excluded. Possible applications of the two combined LDHs are also proposed.

Keywords: layered double hydroxides; wastewater; heavy metals removal

1. Introduction

Layered double hydroxides (LDHs) belong to a family of minerals, the so-called hydrotalcite supergroup, whose crystal structure consists of brucite-type layers, in which a trivalent cation partially substitutes a divalent cation [1,2].

This substitution produces a net positive charge balanced by the entrance of an anionic species in the interlayer, giving as a general formula $M^{2+}_{1-x}M^{3+}_x(A^{z-})_{x/z}(OH)_2 \cdot nH_2O$.

Their capacity to easily exchange the interlayer anions makes LDHs attractive as carriers or scavengers of potential toxic anions [3–6]. Furthermore, their flexible structure, which can be reproduced using several bivalent and trivalent cations, suggests the possibility to use LDHs as a getter of pollutant cations [7,8]. For all of the above, the knowledge of the relationships between metals and LDHs is fundamental to allow the use of these minerals [9].

In a previous study, the relationships between lanthanides metals and a woodwardite (CuAl-SO₄ LDH) structure were investigated [10], with the aim to use these materials for the recovery of the rare earth elements from waste electric and electronic equipment for both georemediation and georecovery exploitation. The aim of this work is the synthesis and characterization of two different LDHs to experimentally investigate their capability to recover pollutants from wastewater. Such wastewater has been taken from a galvanic plant. Its composition is enriched in environmentally hazardous anions

and metal cations, which derive from the treatment process. This problem is widespread [11]. Many different treatments have been proposed to solve this contamination issue [12,13]. In this study, the exchange capability of the two compounds is tested directly on this real wastewater, based on the results previously obtained in a laboratory-prepared $\text{Cr}_2\text{O}_7^{2-}$ solution [14]. The selected compounds are LDHs, as they represent a cheap and effective method to remove pollutants from aqueous solutions. The two compounds investigated are a NiAl- NO_3 and a MgAl- CO_3 LDHs. The choice of these compositions is based on the fact that previous works have shown the chromate uptake capacity by similar LDHs both intercalated with other sorbents [15] and through an ion exchange reaction with the interlayer anion [16,17].

2. Materials and Methods

2.1. Samples Synthesis

The compounds were synthesized via the co-precipitation route (direct method), followed by hydrothermal treatment obtaining nanoscopic crystallites with a partially disordered (turbostratic) structure. The addition of urea to the reactants helps to keep the pH to the desired value and the development of CO_2 allows to obtain a high exchange surface structure [15]. Both the LDHs were with the $\text{M}^{2+}/\text{M}^{3+}$ ratio = 2.

The NiAl- NO_3 LDH was synthesized following the pathway suggested by [18], starting from $\text{Ni}(\text{NO}_3)_2 \cdot 6\text{H}_2\text{O}$ (99.0% purity, supplied by Merck KGaA, Darmstadt, Germany), $\text{Al}(\text{NO}_3)_3 \cdot 9\text{H}_2\text{O}$ (98.8% purity, supplied by VWR CHEMICALS, Leuven, Belgium), and urea (99.8mass% purity, supplied by CARLO ERBA, Milan, Italy). The two salts and urea, in a proper stoichiometric amount, were dissolved in 200 mL of deionized water under magnetic stirring, then the solution was transferred in a Teflon vessel autoclave and kept at 100 °C for 24 h. After heating, the system was cooled at room temperature naturally, and the green solid compound obtained was vacuum filtered and washed with water and ethanol. Subsequently, it was dried in a stove at 60 °C for 24 h. To synthesize the MgAl- CO_3 LDH, as suggested by [19], the reagents $\text{Al}(\text{NO}_3)_3 \cdot 9\text{H}_2\text{O}$ (98.8% purity, supplied by VWR CHEMICALS, Leuven, Belgium), $\text{Mg}(\text{NO}_3)_2 \cdot 9\text{H}_2\text{O}$ (98.9% purity, supplied by VWR CHEMICALS, Leuven, Belgium), and urea (99.8 mass% purity, supplied by CARLO ERBA, Milan, Italy) were used. After the dissolution of the due amount of the reagents, as a function of the Mg/Al desired ratio, the reaction was continued in a Teflon vessel autoclave at 180 °C temperature for one hour. The white compound obtained was separated from the solution by centrifugation at 7000 rpm 10 min^{-1} , repeatedly washed with water, and dried in a stove at 60 °C for 24 h.

2.2. Samples Characterizations

The compounds were characterized by means of the following techniques: thermo gravimetric analysis (TGA), X-ray diffraction analysis on powders (PXRD), field emission scanning electron microscope analysis (FESEM), Fourier transform infrared spectroscopy (FTIR), and inductively coupled plasma optical emission spectroscopy (ICP-OES) chemical analysis.

2.2.1. Thermo Gravimetric Analysis

In order to perform the TGA, about 30–50 mg of the dried powdered LDH was placed in alumina open crucibles; the measurements were carried out by means of a H/LABSYSEVO-1A SETARAM apparatus (Setaram, Caluire, France), at a heating rate of 5 °C min^{-1} under argon flux of 30 mL min^{-1} .

2.2.2. Field Emission Scanning Electron Microscope Analysis

To investigate the morphology and the structure of the synthesized compounds, an FESEM analysis has been performed. The samples were adhered on a conductive resin support, then analyzed by applying an acceleration voltage of 5 kV for 50 s, and a cobalt standard was used for the calibration.

2.2.3. Powder X-ray Diffraction

To determine the crystal structures and to calculate the lattice parameters of the phases, PXRD analysis was carried out by the vertical diffractometer X'Pert MPD (Philips, Almelo, The Netherlands) equipped with a Cu tube ($K\alpha_1$ wavelength: 1.5406 Å). The samples were grounded in an agate mortar. The patterns were collected between 10° and 100° 2θ with a step of 0.001° and measuring time of 50 s/step. The indexing of the obtained diffraction data was performed by a comparison with the literature or calculated data (the program Powder Cell-version1999 [20]).

2.2.4. FTIR Spectroscopy

To exclude the possible incorporation during the synthesis of undesirable anions or other species in the interlayer (e.g., CO_2 from the atmosphere), FTIR spectroscopy was performed using a Spectrum 65 FT-IR Spectrometer (PerkinElmer, Waltham, MA, USA) equipped with a KBr beamsplitter and a DTGS detector by use of an ATR accessory with a diamond crystal. All spectra were recorded from 4000 to 600 cm^{-1} .

2.2.5. Inductively Coupled Plasma Optical Emission Spectroscopy

The chemical analyses were performed by ICP-OES after the dissolution of the samples in the concentrated nitric acid solution.

2.3. Pollutant Removal from Wastewater

Based on the results reported in the literature about the adsorption of anions and cations [7,11], in this work the adsorption efficiency of different pollutants (cationic and anionic) was tested on a real industrial wastewater sample. The sample available was analyzed by means of ICP-OES in order to determine the chemical composition of the dissolved elements. The results are the following: 127 ppm Cu(II), 460 ppm Fe(III), and 8780 ppm Cr(VI). The pH value of the wastewater was about 3. Owing to the very high metals concentration, the sample was diluted to 1/100 with water, before the adsorption tests. The water pH was corrected at a value of about 5 after dilution, to avoid both the LDH dissolution and the iron hydroxide precipitation. For both the LDHs, a weight of 0.5 g of the compound was added to a volume of 100 mL wastewater, and the mixture was shaken for 24 h. The solid and the liquid phases were separated throughout centrifugation at $7000\text{ rpm } 10\text{ min}^{-1}$, then the solid was repeatedly washed with deionized water. The residual wastewater and the solid phase (after dried and acid dissolution) were analyzed by ICP-OES. After the batch equilibration procedure, the pH value of the residual wastewater did not change significantly, and no precipitation of iron hydroxide was observed.

3. Results and Discussions

The compounds were characterized after synthesis and in Figure 1a,b, their PXRD patterns are reported.

Both diagrams had peculiar features of the presence of the LDH structure, such as the strong basal reflections (003 and 006) around 12° and 24° 2θ , respectively. X-ray data confirm the presence of carbonate and nitrate in the two LDHs. The MgAl-CO_3 LDH has an interplanar distance associated with the main basal reflection of 7.54 Å, which is comparable to those of similar natural and synthetic compounds [1,21], whereas the NiAl-NO_3 LDH has an interplanar distance for the (003) reflection of 7.91 Å, as other similar compounds [22]. Comparing the two diagrams, it is also possible to state that the synthesis of the MgAl-CO_3 LDH yielded a material with a crystallite size significantly higher than the NiAl-NO_3 LDH. In fact, the NiAl-NO_3 LDH has broader reflections. Moreover, the PXRD pattern of the NiAl-NO_3 LDH shows a doublet in the (006) reflection, coupled with a diffuse and broad (003) reflection. This is probably due to the different hydration state of this LDH, which leads to the presence of crystallites with small differences in the interlayer distance. Water content is well known to

influence the basal reflection of LDHs, but also the different orientation of nitrate in the interlayer and M^{2+}/M^{3+} ratio could explain this effect [23].

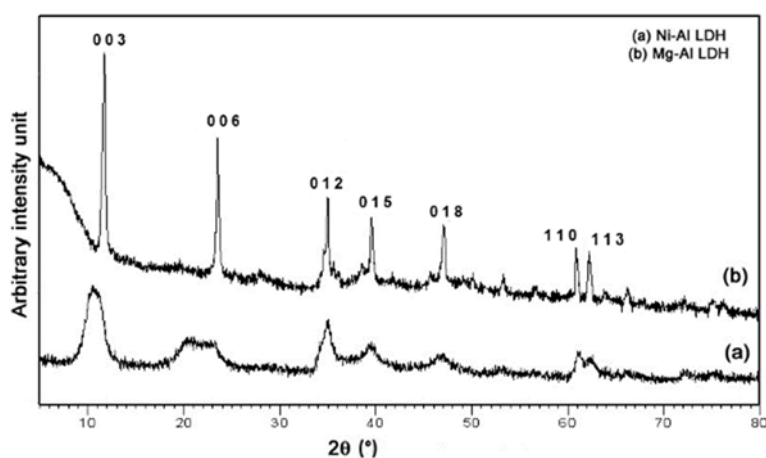


Figure 1. PXRD patterns of (a) NiAl nitrate and (b) MgAl carbonate layered double hydroxides (LDHs). On the graph, the hkl indexes of the main reflections are superimposed.

In Figure 2a,b, the FTIR spectra obtained for the synthesized compounds, the NiAl- NO_3 LDH and MgAl- CO_3 LDH, respectively, are shown, and the presence of the desired functional groups was confirmed.

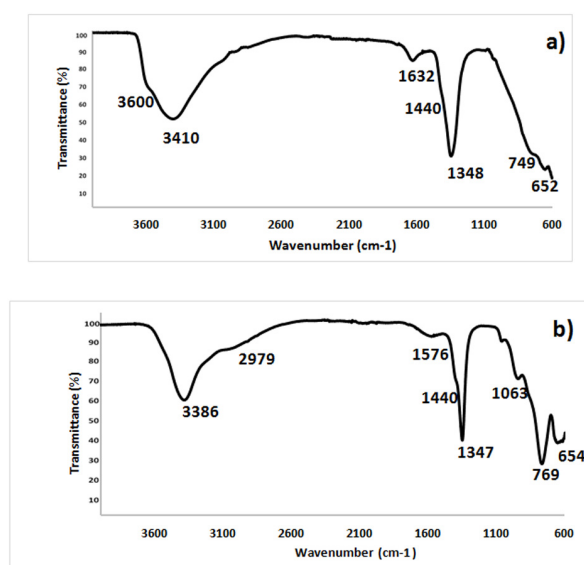


Figure 2. FTIR spectra of (a) the NiAl nitrate LDH, (b) the MgAl carbonate LDH.

Sample (a): A 3600 cm^{-1} OH group stretching, 3410 cm^{-1} hydrogen bond stretching in coordination with the cations, and 1632 cm^{-1} bending of the H_2O bond into the interlayer and at 1348 cm^{-1} can be found in the nitrate group stretching; the two slight bands at 749 and 652 cm^{-1} together with the one at 1440 cm^{-1} partially overlapped with the nitrate bending are related to the undesired interlayer carbonate groups (probably from the atmospheric CO_2). Sample (b): the broad band at 3386 cm^{-1} concerns the stretching of the OH groups in coordination with the cations, at 2979 cm^{-1} there is the large band related to the H-bonding between the water and carbonate anions in the interlayer, the 1576 cm^{-1} band originates from the H_2O bending in the interlayer, and the main carbonate anion adsorption band at 1440 cm^{-1} is overlapped with the 1347 cm^{-1} band related to the nitrate group

stretching; ongoing to the lower frequency at 1063 cm^{-1} , there is the signal due to the carbonate vibration and the two bands at 769 and 654 cm^{-1} are related to the interlayer carbonate groups.

From these spectra, it seems that in the MgAl carbonate LDH there are some impurities of the nitrate anions, while the NiAl LDH is affected by a little impurity of carbonate.

The FESEM images are shown in Figure 3a,b, and from the micrographic appearance, the two structures appear similar in morphology, showing the typical hydroxylate structure, and the thickness of the constituent lamellae was estimated between 10 and 20 nm.

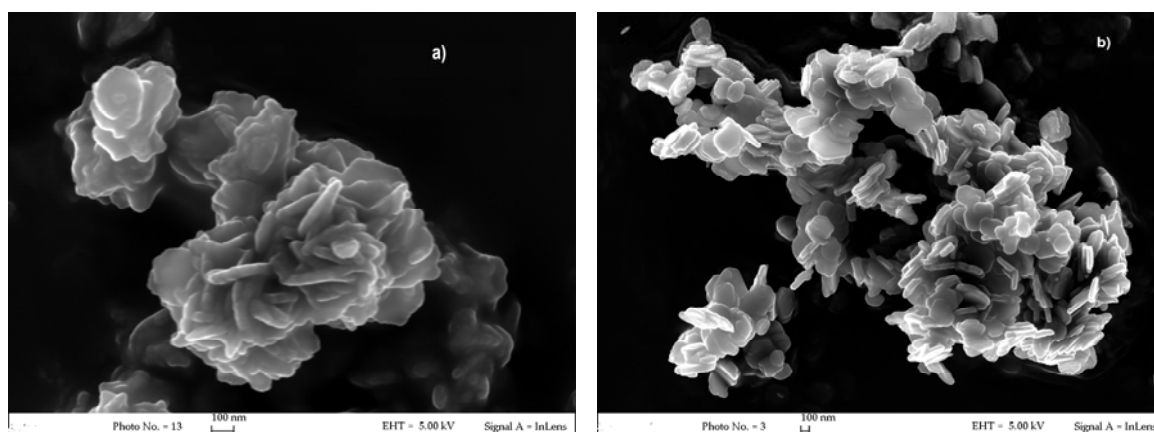


Figure 3. FESEM images of (a) the NiAl-NO₃ LDH, (b) the MgAl-CO₃ LDH.

For the NiAl-NO₃ LDH the specific surface area, calculated by the Brunauer–Emmett–Teller (BET) method, has been measured, resulting in $46.8504\text{ m}^2\text{ g}^{-1}$.

The thermogravimetric analysis, whose results are reported in Figure 4a,b, revealed that the NiAl-based LDH (Figure 4a) loses 2.7 mass% due to humidity at about $150\text{ }^\circ\text{C}$, and has a second mass decreasing at $309.3\text{ }^\circ\text{C}$, involving both the interlayer water and the nitrogen oxide for a whole amount of 24.7 mass%. The MgAl-based LDH (Figure 4b) loses mass in three steps. The first, due to humidity, at $231\text{ }^\circ\text{C}$ with a mass decrease of 10 mass%, the second ascribable to the removal of the interlayer water (6.5 mass% loss at $328\text{ }^\circ\text{C}$), and the third of about 16 mass% was due to the CO₂ loss, which started at about $400\text{ }^\circ\text{C}$.

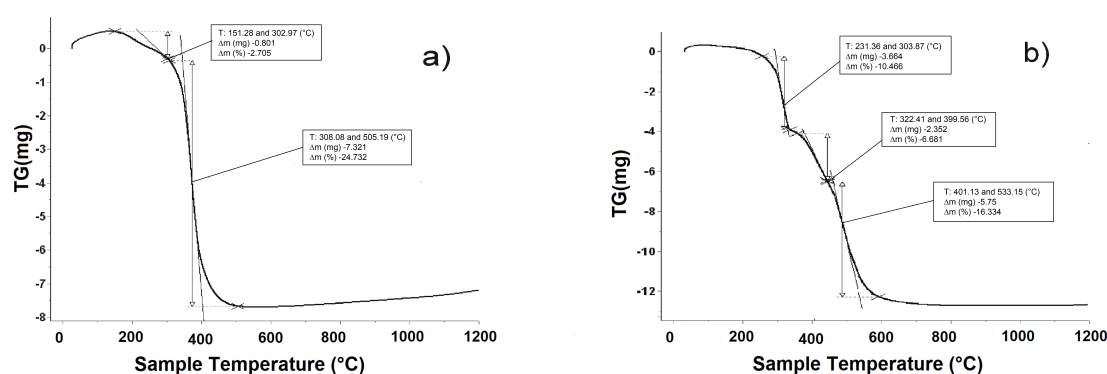


Figure 4. TG thermograms of (a) the NiAl nitrate LDH, (b) the MgAl carbonate LDH.

As the pollutant removal, both the samples have been kept to a batch equilibration with the wastewater, in the experimental conditions previously described. In Tables 1 and 2, the results obtained for the extraction of copper, iron, and chromium, the three pollutants of the industrial wastewater, are reported.

Table 1. Pollutant amount in the diluted wastewater before and after treatment with the NiAl-NO₃ LDH.

Pollutant	Concentration [ppm]			Recovery Efficiency
	Diluted Water		LDH	
	before treatment	after treatment	after water treatment	
Cu(II)	1.27	0.57	32	25.2
Fe(III)	4.60	0.51	112	24.3
Cr(VI)	87.8	1.18	6840	77.9

Table 2. Pollutant amount in the diluted wastewater before and after treatment with the MgAl-CO₃ LDH.

Pollutant	Concentration [ppm]			Recovery Efficiency
	Diluted Water		LDH	
	before treatment	after treatment	after water treatment	
Cu(II)	1.27	0.01	220.0	173
Fe(III)	4.60	0.02	4700.0	1021
Cr(VI)	87.8	62.0	2370	27

In the tables, the concentration of the three species investigated in the wastewater, before and after the adsorption procedure, and in the solid LDH used to extract the pollutants are shown. The recovery efficiency value expresses the ratio of the element concentration in the LDH to the element concentration in the medium, calculated in each test [24].

The NiAl-NO₃ compound demonstrated greater affinity for the CrO₄²⁻ anion than for the Fe(III) and Cu(II) cations. On the contrary, the MgAl-CO₃ structure did not adsorb significantly the CrO₄²⁻ anion, while it seemed more useful for the two cations.

The chromium adsorption is related to the different exchange capacity of the two anions (CO₃²⁻ and NO₃⁻) in the interlayers, where nitrate can be easily substituted by chromate, as confirmed from the PXRD. The comparison between the position of the three main reflections of the compound before and after the chromium extraction from the water are reported in Figure 5. The shift of the main basal reflections of the NiAl LDH toward lower 2θ values (Figure 5a) indicates an enlargement of the interlayers due to the substitution of NO₃⁻ with CrO₄²⁻. This shift is reflected in a change in the cell parameter *c* (calculated as $c = 3 \times d_{(003)}$), which changed from 23.85 to 24.99 Å, caused by the swelling of the interlayer due to the NO₃⁻ with CrO₄²⁻ substitution. The low crystallinity of the samples prevented to meaningfully discuss the cell parameter *a*, calculated as $a = 2 \times d_{(110)}$.

The values of the cell parameter *c* of the MgAl-CO₃ LDHs before and after the experiment are 22.71 and 22.56 Å, respectively. This fact suggests that little changes took place in the interlayer of these LDHs, as confirmed by Figure 5b. The high affinity of the MgAl-CO₃ LDH for the two cations is worthy of further study, but as for copper, it seems to be imputable to an exchange between the copper and magnesium divalent cations due to the similar ionic radius values of the two elements in octahedral coordination (72 and 73 pm, respectively). No significant change in the *a* parameter before and after the experiment is observed, as its value remains constant at 3.04 Å. Probably, the disordered nature of the cation arrangement in the brucite-like layers prevents the observation of the changes in the *a* parameter [2]. The Cu-Mg substitution has already been proposed for MgAl LDHs in contact with solutions in which bivalent cations are dissolved [25], even if sorption on the OH⁻ functional groups, surface complexation, and/or precipitation of small amounts of Me(OH)₂ on the surface of the MgAl LDH could not be completely excluded [9]. Regarding iron adsorption, the characterization analysis did not provide precise information on where it might have accumulated. It is possible that Fe has been removed via interaction with the functional groups on the surface of the mineral.

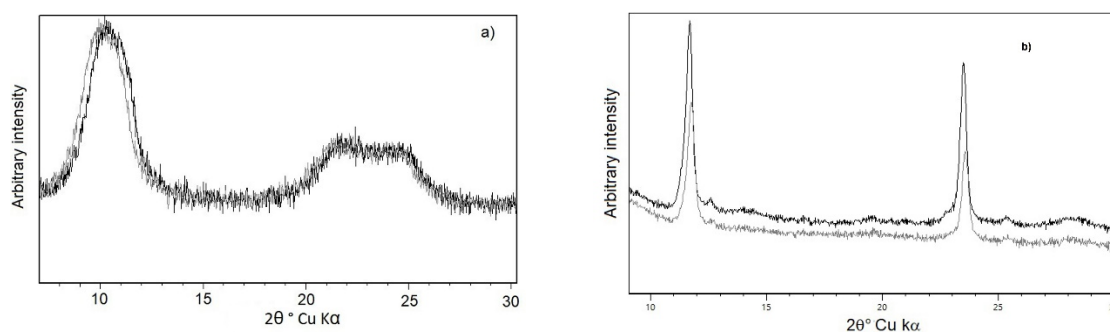


Figure 5. PXRD for (a) the NiAl nitrate LDH before (dark grey) and after (light grey) pollutant removal from the wastewater and (b) the MgAl carbonate LDH before (dark grey) and after (light grey) pollutant removal from the wastewater.

4. Conclusions

The experimental results obtained lead to the following conclusions:

- The LDHs' syntheses are relatively easy to prepare, leading to the required products as shown by the characterization analyses conducted;
- As the tested LDHs:
- The NiAl-NO₃ compound demonstrates greater affinity for the CrO₄²⁻ anion than for the Fe(III) and Cu(II) cations;
- The MgAl-CO₃ structure does not significantly adsorb the CrO₄²⁻ anion, while it seems more effective for the two cations;
- By comparing the residual concentration of the three elements studied with the Italian legal limit for industrial wastewater, reported in Table 3, with respect to the disposal in superficial water or in the drainage system:

Table 3. Italian legal concentration limit for chromium (VI), iron, and copper for disposal in both superficial water and drainage systems. (All. 5, P. Terza, D. Lgs n.152 del 03-04-06).

Element	Superficial Water/ppm	Drainage System/ppm
Cu(II)	0.1	0.4
Fe(III)	2.0	4.0
Cr(VI)	0.2	0.2

The NiAl-NO₃ compound reduces the Cr(VI) content at a value close to the legal limit, but is not sufficiently low. Some improvements of the methods (reaction time, sorbent/wastewater ratio) could help in reaching the goal.

The MgAl-CO₃ LDH demonstrates to be very effective in lowering the Cu(II) and Fe(III) concentration to below the legal limit.

For all of the above, the next step will be to test the effectiveness of a combined use of the two metal getters and their transformation into a spinel-like structure after heating for a potential reuse.

Author Contributions: Conceptualization: A.M.C., C.C.; investigation: A.M.C., S.C., M.F., N.P.; methodology: A.M.C., S.C.; writing—original draft preparation: A.M.C., S.C.; writing—review and editing: A.M.C., S.C.; resources: A.M.C., C.C. All authors have read and agreed to the published version of the manuscript.

Funding: This research received no external funding.

Conflicts of Interest: The authors declare no conflict of interest.

References

1. Mills, S.J.; Christy, A.G.; Génin, J.-M.R.; Kameda, T.; Colombo, F. Nomenclature of the hydrotalcite supergroup: Natural layered double hydroxides. *Miner. Mag.* **2012**, *76*, 1289–1336. [[CrossRef](#)]
2. Evans, D.G.; Slade, R.C.T. *Layered Double Hydroxides*; Duan, X., Evans, D.G., Eds.; Springer: Berlin/Heidelberg, Germany, 2006; Chapter 1; pp. 1–87. ISBN 978-3-540-28279-2.
3. Wang, Y.; Gao, H. Compositional and structural control on anion sorption capability of layered double hydroxides (LDHs). *J. Colloid Interface Sci.* **2006**, *301*, 19–26. [[CrossRef](#)] [[PubMed](#)]
4. Morimoto, K.; Anraku, S.; Hoshino, J.; Yoneda, T.; Sato, T. Surface complexation reactions of inorganic anions on hydrotalcite-like compounds. *J. Colloid Interface Sci.* **2012**, *384*, 99–104. [[CrossRef](#)]
5. Golban, A.; Lupa, L.; Cocheci, L.; Rodica, P. Synthesis of MgFe Layered Double Hydroxide from Iron-Containing Acidic Residual Solution and Its Adsorption Performance. *Crystals* **2019**, *9*, 514. [[CrossRef](#)]
6. Dore, E.; Frau, F.; Cidu, R. Antimonate Removal from Polluted Mining Water by Calcined Layered Double Hydroxides. *Crystals* **2019**, *9*, 410. [[CrossRef](#)]
7. Mishra, G.; Dash, B.; Pandey, S. Layered double hydroxides: A brief review from fundamentals to application as evolving biomaterials. *Appl. Clay Sci.* **2018**, *153*, 172–186. [[CrossRef](#)]
8. Tamzid Rahman, M.; Kameda, T.; Kumagai, S.; Yoshioka, T. A novel method to delaminate nitrate-intercalated MgAl layered double hydroxides in water and application in heavy metals removal from waste water. *Chemosphere* **2018**, *203*, 281–290. [[CrossRef](#)]
9. Liang, X.; Zang, Y.; Xu, Y.; Tan, X.; Hou, W.; Wang, L.; Sun, Y. Sorption of metal cations on layered double hydroxides. *Colloids and Surfaces A: Physicochem. Eng. Asp.* **2013**, *433*, 122–131. [[CrossRef](#)]
10. Consani, S.; Balić-Žunić, T.; Cardinale, A.M.; Sgroi, W.; Giuli, G.; Carbone, C. A Novel Synthesis Routine for Woodwardite and Its Affinity towards Light (La, Ce, Nd) and Heavy (Gd and Y) Rare Earth Elements. *Materials* **2018**, *11*, 130. [[CrossRef](#)]
11. Zinicovskaia, I.; Safonov, A.V.; Khijniak, T.V. *Heavy Metals and Other Pollutants in the Environment: Biological Aspects*; Zaikov, G.E., Weisfeld, L.I., Lisitsyn, E.M., Bekuzarova, S.A., Eds.; Apple Academic Press: Waretown, NJ, USA, 2017; Chapter 17; pp. 333–360. ISBN 978-1-315-36602-9.
12. Kobya, M.; Erdem, N.; Demirbas, E. Treatment of Cr, Ni and Zn from galvanic rinsing wastewater by electrocoagulation process using iron electrodes. *Desalin. Water Treat.* **2014**, *56*, 1191–1201. [[CrossRef](#)]
13. Bednarik, V.; Vondruska, M.; Koutny, M. Stabilization/solidification of galvanic sludges by asphalt emulsions. *J. Hazard. Mat.* **2005**, *B122*, 139–145. [[CrossRef](#)] [[PubMed](#)]
14. Goswamee, R.L.; Sengupta, P.; Bhattacharyya, K.G.; Dutta, D.K. Adsorption of Cr(VI) in layered double hydroxides. *Appl. Clay Sci.* **1998**, *13*, 21–34. [[CrossRef](#)]
15. Chen, S.; Huang, Y.; Han, X.; Wu, Z.; Lai, C.; Wang, J.; Deng, Q.; Zeng, Z.; Deng, S. Simultaneous and efficient removal of Cr(VI) and methyl orange on LDHs decorated porous carbons. *Chem. Eng. J.* **2018**, *352*, 306–315. [[CrossRef](#)]
16. Chao, H.-P.; Wang, Y.-C.; Tran, H.N. Removal of hexavalent chromium from groundwater by Mg/Al-layered double hydroxides using characteristics of in-situ synthesis. *Environ. Pollut.* **2018**, *243*, 620–629. [[CrossRef](#)]
17. Lei, C.; Zhu, X.; Zhu, B.; Jiang, C.; Le, Y.; Yu, J. Superb adsorption capacity of hierarchical calcined Ni/Mg/Al layered double hydroxides for Congo red and Cr(VI) ions. *J. Hazard. Mat.* **2017**, *321*, 801–811. [[CrossRef](#)]
18. Liu, H.; Yu, T.; Su, D.; Tang, Z.; Zhang, J.; Liu, Y.; Yuan, A.; Kong, Q. Ultrathin NiAl layered double hydroxide nanosheets with enhanced supercapacitor performance. *Ceram. Int.* **2017**, *43*, 14395–14400. [[CrossRef](#)]
19. Rao, M.M.; Reddy, B.R.; Jayalakshmi, M.; Jaya, V.S.; Sridhar, B. Hydrothermal synthesis of Mg–Al hydrotalcites by urea hydrolysis. *Mat. Res. Bull.* **2005**, *40*, 347–359. [[CrossRef](#)]
20. Kraus, W.; Nolze, G. *Powder Cell for Windows*; Federal Institute for Materials Research and Testing: Berlin, Germany, 1999.
21. Somosi, Z.; Muráth, S.; Nagy, P.; Sebők, D.; Szilagy, I.; Douglas, G. Contaminant removal by efficient separation of in situ formed layered double hydroxide compounds from mine wastewaters. *Environ. Sci. Water Res. Technol.* **2019**, *5*, 2251–2259. [[CrossRef](#)]
22. Ravuru, S.S.; Jana, A.; De, S. Synthesis of NiAl- layered double hydroxide with nitrate intercalation: Application in cyanide removal from steel industry effluent. *J. Hazard. Mater.* **2019**, *373*, 791–800. [[CrossRef](#)]
23. Marappa, S.; Radha, S.; Kamath, P.V. Nitrate-intercalated layered double hydroxides—Structure model, order, and disorder. *Eur. J. Inorg. Chem.* **2013**, *2013*, 2122–2128. [[CrossRef](#)]

24. Jakubiak, M.; Giska, I.; Asztemborska, M.; Bystrzejewska-Piotrowska, G. Bioaccumulation and biosorption of inorganic nanoparticles: Factors affecting the efficiency of nanoparticle mycoextraction by liquid-grown mycelia of *Pleurotus eringi* and *Trametes versicolor*. *Mycol. Progress.* **2013**, *13*, 525–532. [[CrossRef](#)]
25. González, M.A.; Pavlovic, I.; Barriga, C. Cu(II), Pb(II) and Cd(II) sorption on different layered double hydroxides. A kinetic and thermodynamic study and competing factors. *Chem. Eng. J.* **2015**, *269*, 221–228. [[CrossRef](#)]



© 2020 by the authors. Licensee MDPI, Basel, Switzerland. This article is an open access article distributed under the terms and conditions of the Creative Commons Attribution (CC BY) license (<http://creativecommons.org/licenses/by/4.0/>).